River Flow 2010 - Dittrich, Koll, Aberle & Geisenhainer (eds) - © 2010 Bundesanstalt für Wasserbau ISBN 978-3-939230-00-7

Reach-Scale Resistance of Distributed Roughness in Channels

C. S. James
Centre for Water in the Environment, School of Civil & Environmental Engineering, University of the Witwatersrand, Private Bag 3, Wits, 2050 South Africa

A. A. Jordanova
Golder Associates Africa (Pty) Ltd, P O Box 6001, Halfway House, 1685, South Africa

ABSTRACT: Appropriate description of flow resistance in a river depends on the purpose of the description, the information available, and how the underlying processes are accounted for. For 1D reach-scale modelling, a lumped resistance coefficient such as Manning's n is widely used. Estimating this coefficient requires either direct calibration, use of previously determined and documented values, or synthesis by combining known individual effects of smaller scale channel characteristics. These characteristics include surface roughness and discrete features, which may be nonuniformly distributed over the reach. Results from experiments with nonuniformly distributed surface roughness, vegetation and large emergent features are used to test formulations for combining local resistance effects. Results show that for spatially distributed surface roughness an overall Manning's n can be reliably calculated as a combination of local values weighted by their contributing areas. Resistance originating from both form and surface drag cannot be combined in this way and a rational combination equation is shown to be effective. This equation is used to show that calculating a combined Manning's n as the square root of the sum of the squares of constituent values is preferable to the practice of adding modifying values to a basic surface n value.

Keywords: River flow, Flow resistance, Hydraulic roughness

1 INTRODUCTION

The flow resistance of a river is an expression of the effects that its physical features have on its flow characteristics. While the fundamental underlying phenomena can only be explained through high resolution analysis, their effects are manifest and can be pragmatically accounted for over a range of scales and levels of resolution. The level most appropriate for description and quantification of resistance depends on the purpose of the analysis, the type and amount of information available, and the way in which the underlying processes are accounted for.

The types of problems requiring description of resistance range from defining stage-discharge relationships at the broadest level to describing velocity and shear distributions in three dimensions at high resolutions. The information available at any level is of two types, describing flow characteristics and physical channel characteristics. At any level of description, the processes underlying observable flow characteristics are accounted for by both deterministic modelling and empirical correlation. As the required resolution of flow description increases, the verisimilitude of process modelling improves while the degree of dependence on empirical input decreases. Correspondingly, less flow information is required for calibration, but more physical information is required for characterizing the channel; models become more general and less site-specific, but not necessarily more accurate, as resolution increases. At any particular level, the model used will describe the processes observable at that level and account for effects of finer resolution processes through an appropriate resistance coefficient. So, for example, a 1D model for describing cross-section average flow characteristics through a river bend will incorporate a resistance coefficient that accounts for the effect of secondary circulation, while a 3D model for predicting local variations will describe the circulation explicitly and incorporate a different resistance coefficient that accounts only for even finer resolution processes.

Description of resistance is therefore particular to the level of resolution addressed by the model used. A drag coefficient, for example, only has meaning if the model recognises discrete roughness elements. At finer resolutions the boundary shear and pressure distributions would be described over a continuous surface; at coarser resolutions the drag would be lumped together with other resisting effects. At each level, the required resistance coefficient can be obtained directly by calibration, from empirical relationships obtained from measurements of flow and physical characteristics at that level, or by synthesizing values using higher resolution descriptions. A drag coefficient could be determined by correlating measured drag forces with approach velocities or by integrating pressure and shear distributions obtained by higher resolution measurement or modelling.

Many engineering and environmental problems in rivers are most appropriately addressed through analysis at the river reach level, using 1D models that do not describe explicitly the finer scale processes that influence resistance as perceived at the analysis scale. Manning's equation remains the most widely used for expressing resistance at this level, i.e.

$$V = \frac{1}{n} R^{2/3} S^{1/2} \tag{1}$$

where V = the cross-section average velocity, R = the hydraulic radius, n = the resistance coefficient, and S = the channel slope (for uniform flow).

Although the form of this equation reflects only the influence of boundary shear on flow depth and average velocity, the resistance coefficient, n, has come through common usage to be a lumped parameter accounting for all the various influences in a river reach. It is best calibrated directly, but is commonly estimated through experience, aided by previously determined correlations with physical channel characteristics documented as verbal descriptions or photographs. Such an approach is confounded by uncertainty and apparently inconsistent variations with flow conditions. Alternative or complementary methods have therefore been proposed for synthesizing resistance coefficient values from knowledge of the separate, smaller scale contributing effects. This work aims to develop this approach, and is especially directed at low flow conditions where the resistance coefficient is particularly sensitive to variations of flow depth. It is intended particularly to facilitate environmental flow assessments in South Africa, where opportunities are very limited for collecting either sufficient flow information for direct calibration of resistance coefficients at the reach scale or sufficient physical channel information for application of higher resolution models.

Various methods have been suggested for synthesizing a composite resistance coefficient. Where only surface roughness contributes to resistance, but the roughness size varies across the channel cross section (but not longitudinally), a number of formulations for calculating the overall, effective value of Manning's n (n_e) have been proposed. These can be expressed as weighted averages of functions of local n values, i.e.

$$n_e = \left(\frac{\sum_{i=1}^{N} \left(K_i \, n_i^a \right)}{K} \right)^{1/a} \tag{2}$$

where the subscript i refers to the subsection associated with the local value n_i, N = the number of subsections specified, K = the weighting variable (usually the wetted perimeter, P), and a = an exponent which depends on the nature of the relationship assumed between subsection flow conditions. The most commonly used expressions of Eq. (2) are those of Pavlovski (1931) who proposed a = 2 and Horton (1933) who proposed a = 3/2. Such formulations do not account for the interaction between subsection flows through transverse momentum exchange, which is considerable for overbank flows but less influential for most low, inbank flows. The effect of this interaction can be accounted for using a lateral distribution model, such as is incorporated in the Conveyance Estimation System produced by HR Wallingford (2004), although this application depends on local composite unit roughnesses, n_l, (analogous to Manning's n) evaluated by the largely intuitive formula

$$n_l = \left(n_{sur}^2 + n_{veg}^2 + n_{irr}^2 \right)^{1/2} \tag{3}$$

in which n_{sur} accounts for surface roughness, n_{veg} for vegetation and n_{irr} for irregularity.

Equation (3) is intended for use at the local, sub-cross section scale. For reach scale applications, and with roughness variations not restricted to the transverse direction, the United States Soil Conservation Service (1963) proposed an equation for the overall Manning coefficient (based on a concept introduced by Cowan (1956)) in which a basic value associated with the channel surface (n_b) is augmented by modifying values to account for surface irregularity (n_1), cross-section size and shape variations (n_2), obstructions (n_3), vegetation (n_4) and meandering (m), i.e.

$$n_e = \left(n_b + n_1 + n_2 + n_3 + n_4\right) m \quad (4)$$

Equations (3) and (4) both include terms to account for resistance originating from form and surface drag. These phenomena are different in nature and produce effects that vary differently with flow depth. They should therefore be described in different terms. James et al. (2008) proposed Eq. (5) for combining local form and bed shear contributions to resistance. This equation is derived from the balance of forces on a control volume in the flow, these being the downslope weight component of the water, the drag exerted by discrete elements extending through the full flow depth, and the shear acting at the bed surface between the discrete elements. The equation was originally developed for combined vegetation stem and bed resistance, but can also be applied at the channel reach scale to account for large emergent roughness elements such as boulders.

$$V = \sqrt{\frac{1}{C_S + C_D}} \sqrt{2 g l S} \quad (5)$$

In this equation l = a roughness length related to the spacing (s) and width (d) of form roughness elements by

$$l = \frac{s^2}{d} \quad (6)$$

Form resistance is accounted for by a drag coefficient (C_D) and the bed shear resistance by the term C_S, which can be expressed in terms of the local surface Darcy-Weisbach f or Manning n by

$$C_S = \frac{f l}{4D} = \frac{2 g l n^2}{D^{4/3}} \quad (7)$$

in which D = the flow depth and g = gravitational acceleration.

The different ways of combining resistance contributions have been tested against laboratory experimental results. Four situations involving spatially distributed surface and form elements were considered: a) channels with different surface roughnesses distributed both longitudinally and transversely, b) channels with strips of emergent vegetation, especially along their banks, c) channels with distributed patches of emergent vegetation, and d) channels with combined surface roughness and discrete, solid, form roughness-inducing elements. The experiments were conducted with spatially uniform flow depths and only two roughness types in combination in each situation, although the formulations used could be extended to more types.

2 SPATIALLY DISTRIBUTED SURFACE ROUGHNESS

The conventional composite roughness formula (Eq. (2)) and lateral distribution models account for transverse roughness variations across the width of a channel, rather than longitudinal or two-dimensional variations in plan. Bhembe and Pandey (2006) investigated the effects of more general roughness distribution patterns and ways of accounting for them. Their experiments were done in a 12.0 m long, 2.0 m wide flume on a slope of 0.0005. The roughness patterns shown in Fig. 1 were created by arranging 0.50 m square steel panels onto which were glued fine gravel particles with d_{50} = 6.7 mm. Experiments with 0% and 100% rough surface coverage indicated

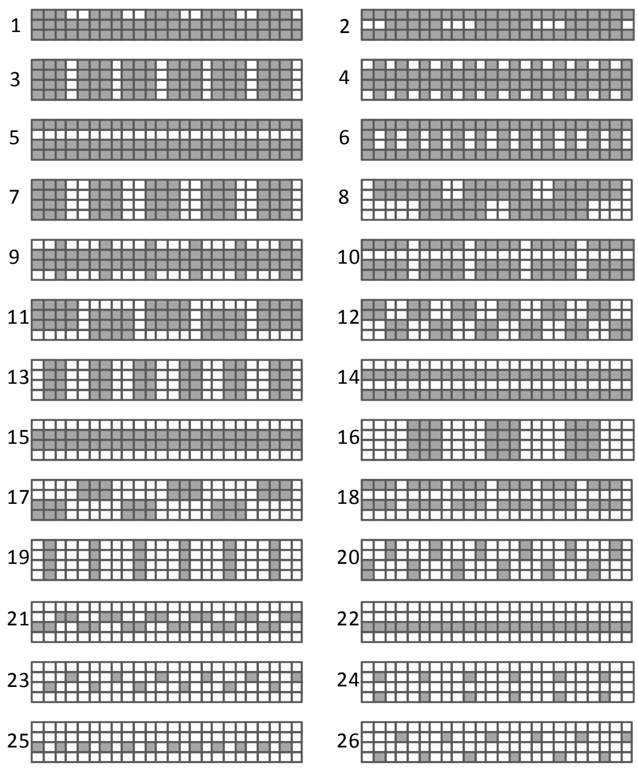

Figure 1. Spatially distributed surface roughness patterns tested by Bhembe and Pandey (2006). (Shaded panels are rough, unshaded are smooth.)

Manning's n values for the smooth and rough surfaces of 0.0107 and 0.0216 respectively. Each pattern was tested with a single discharge producing a uniform flow depth between 0.05 m and 0.08 m. For each case, the overall value of Manning's n (n_e) was calculated from the measured discharge and flow depth, and also estimated using Eq. (2) with $K = A$, the surface area, to allow application to the channel reach rather than just the cross section. (For purely longitudinal strip patterns this reduces to using $K = P$.) Exponent values of a = 2, 3/2 and 1 were tested.

Equation (2) with $K = A$ and the three values of a all predicted the composite Manning's n adequately, with a = 1 performing slightly better than the others. The average absolute errors in predicted n_e values for all the roughness patterns are 0.0013, 0.0011 and 0.00093 for a = 2, 3/2 and 1 respectively. The corresponding average absolute errors in calculated discharge are 7.53%, 6.08% and 5.57%. Values of n_e predicted with a = 1 are compared with the measured values in Fig. 2. Interestingly, the greatest errors for all the equations were for the longitudinal strip patterns, the situation for which a = 2 and 3/2 were actually proposed by Pavlovski (1931) and Horton (1933).

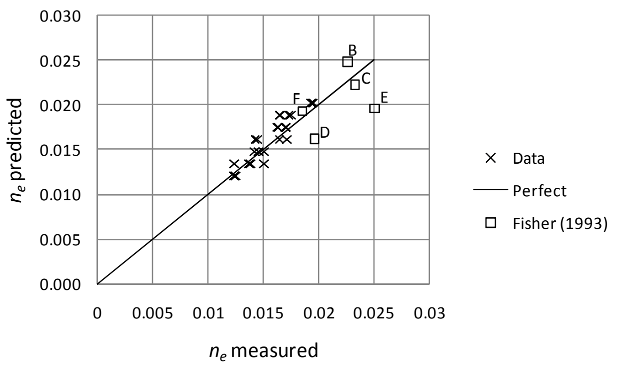

Figure 2. Overall Manning's n values for spatially distributed surface roughness predicted by Eq. (2) with $K=A$ and a = 1.

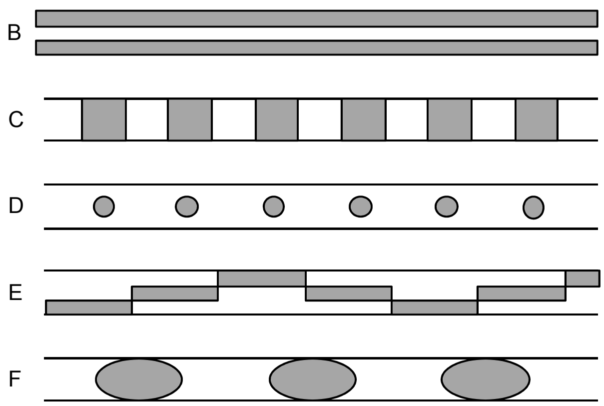

Figure 3. Surface roughness patterns investigated by Fisher (1993) shown over part of the flume length.

Fisher (1993) carried out similar experiments with some rather different patterns in a 25 m long, 0.9 m wide flume on a gradient of 0.000865. The roughness patterns shown in Fig. 3 were formed by a single layer of 10 mm gravel and repeated to extend over the full length of the flume. The longitudinal strips in pattern B were 0.33 m wide, providing an areal coverage of 67%. The lengths and spacings of the square patches in pattern C were 1.0 m, giving an areal coverage of 50%. The circular patches in pattern D were 0.5 m in diameter and placed at 2.0 centre spacings, giving an areal coverage of 10.7%. The rectangular patches in pattern E were 0.3 m wide and 2.0 m long, resulting in an areal coverage for the whole pattern of 33%. The patches in pattern F were elliptical with major axes of 2.0 m and minor axes of 0.9 m, and were spaced 2.0 m apart, giving an areal coverage over the entire flume length of 30.8%. Tests on the smooth flume bed and a fully rough bed gave n values of 0.0146 and 0.0299. Several discharges were tested on each pattern, but only the n_e values obtained for a common discharge of 0.05 m^3/s are used in this analysis to maintain consistency (as also done by Fisher).

As for the previous data set, Eq. (2) was applied to Fisher's (1993) conditions, with $K = A$ and a = 2, 3/2 and 1. Average absolute errors in n_e prediction for the three a values are similar, i.e. 0.00249, 0.00248 and 0.00257. The values predicted with a = 1 are compared with the measured values in Fig. 2. The corresponding average absolute errors in calculated discharge are 11.9%, 12.3% and 13.2%. Predictions are more accurate for patterns B, C and F than for patterns D and E. This indicates a likely influence of pattern shape on resistance, although the measured energy gradients for some experiments were rather different from the bed slope (ranging between 0.000462 and 0.00134) and the resulting flow nonuniformity might also have had some influence.

3 EMERGENT BANK VEGETATION

The resistance phenomena within emergent vegetation and over rough surfaces are so different in nature and magnitude that it is sensible to treat separately the different channel areas where they occur, if their spatial arrangements so permits. This is the case with strips of emergent vegetation (such as reeds) along the banks of rivers, and a zonal approach is recommended for estimating conveyance, with discharge calculated separately for the vegetated and clear zones and then added. James and Makoa (2006) conducted experiments with longitudinal strips of artificial vegetation in a 12.3 m long, 1.0 m wide, plaster-lined channel on a slope of 0.00107. The vegetation stems were represented by 5 mm diameter rods mounted in 1.0 m by 0.125 m frames in a staggered arrangement with centre spacings of 25 mm in both the longitudinal and transverse directions. The frames were arranged in longitudinal strips with seven different widths and locations, each covering 50% of the channel area. Some patterns had strips on both sides of clear zones and these can be interpreted as channels with bank strips. Those patterns producing realistic width to depth ratios (W/D) (greater than about 2) were selected for analysis and are shown in Fig. 4. The value of n for the flume surface was found from a test with no stems to be 0.0102. A value of 0.0432 was found for the stem-water interfaces through application of a sidewall correction procedure using discharges determined from integrated velocity measurements across the clear sections. Each strip pattern was tested with four or five different discharges.

Figure 4. Artificial emergent vegetation strip patterns selected from those tested by James and Makoa (2006).

The effective resistance of clear channels between vegetation strips can be described by composite roughness equations. Equation (2) was applied with $K = P$ and $a = 2$, 3/2 and 1. The relative contribution of the side boundaries to the overall resistance (n_e) decreases as W/D increases; this effect was described adequately by the composite equation with all three a values (Fig. 5). The average absolute errors in discharge predictions using n_e calculated with $a = 2$, 3/2 and 1 are 10.2%, 4.7% and 13.0% respectively. Horton's (1933) equation ($a = 3/2$) is therefore the best of those tested.

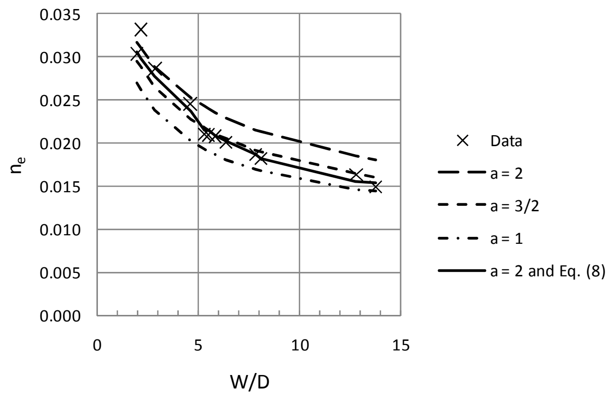

Figure 5. Variation of predicted and measured overall Manning's n values with width to depth ratio for channels with emergent bank vegetation.

Hirschowitz and James (2009) developed this approach further, using the Darcy-Weisbach friction factor, f, rather than n and with $a = 1$ (which is equivalent to using n with $a = 2$). For the stem-water interface friction factor, f_v, they recommend an equation proposed by Kaiser (1984), i.e.

$$f_v = f_{To} + 0.18\log\left(0.0135\frac{V_{\inf}^2}{h_T\,V_{veg}^2}\right) \tag{8}$$

in which V_{inf} = the depth-averaged velocity in the channel as unaffected by vegetation, V_{veg} = the depth-averaged velocity within the vegetated zone (to be calculated using Eq. (5)), h_T = the flow depth, and f_{To} = a constant which Hirschowitz and James (2009) recommend to be equal to zero for W/D greater than about 5 and between 0.06 and 0.1 for narrower channels. This procedure improves the predicted variation of n_e with W/D (Fig. 5) resulting in predictions of discharges for Patterns 1, 3 and 5 with an average absolute error of 2.6%. The improvement in performance made by this modification suggests that the variation of resistance of the stem-water interface with flow condition probably accounts for more error than the value of a selected.

4 SPATIALLY DISTRIBUTED PATCHES OF EMERGENT VEGETATION

Vegetation in rivers does not always occur in strips along the banks, but may be dispersed in patches over a reach area. Vegetation that is completely submerged by relatively deep flow will contribute to resistance in the same way as a rough bed, and patches can be treated as for the distributed surface roughness described above. Emergent vegetation patches experience internal form resistance, for which the local n value varies significantly with flow depth. James et al. (2001) tested a number of spatially distributed patterns created with the same artificial vegetation units used for the longitudinal strip experiments and in the same channel as described above (Fig. 6).

The approach followed for predicting the overall Manning's n was to use the same equations as for the spatially distributed surface roughness case (i.e. Eq. (2) with $K = A$, and $a = 2$, 3/2 and 1) to account for the overall vegetation coverage, and Eqs (5), (6) and (7) with $C_D = 1$ to determine the local vegetative resistance at different flow depths. For this situation the performance of the different composite roughness equations is very different. Average absolute errors in prediction of n_e are 0.023, 0.071 and 0.0068 with $a = 2$, 3/2 and 1 respectively. The values predicted with $a = 1$ are thus significantly better than with the others, and are compared with the measured values in Fig. 7. The corresponding average absolute errors in discharge prediction are 38.5%, 65.5% and 16.9%.

Although the performance of Eq. (2) with $a = 1$, together with Eqs (5) to (7), is not good overall, it varies considerably with the pattern of vegetation patch distribution, being very good for evenly distributed, small patches but less so for large patches where performance deteriorates with increasing flow depth. The overall resistance in this case is therefore not simply a superposition of independent contributions in proportion to their preponderance, but includes an emergent effect associated with the pattern of the roughness distribution.

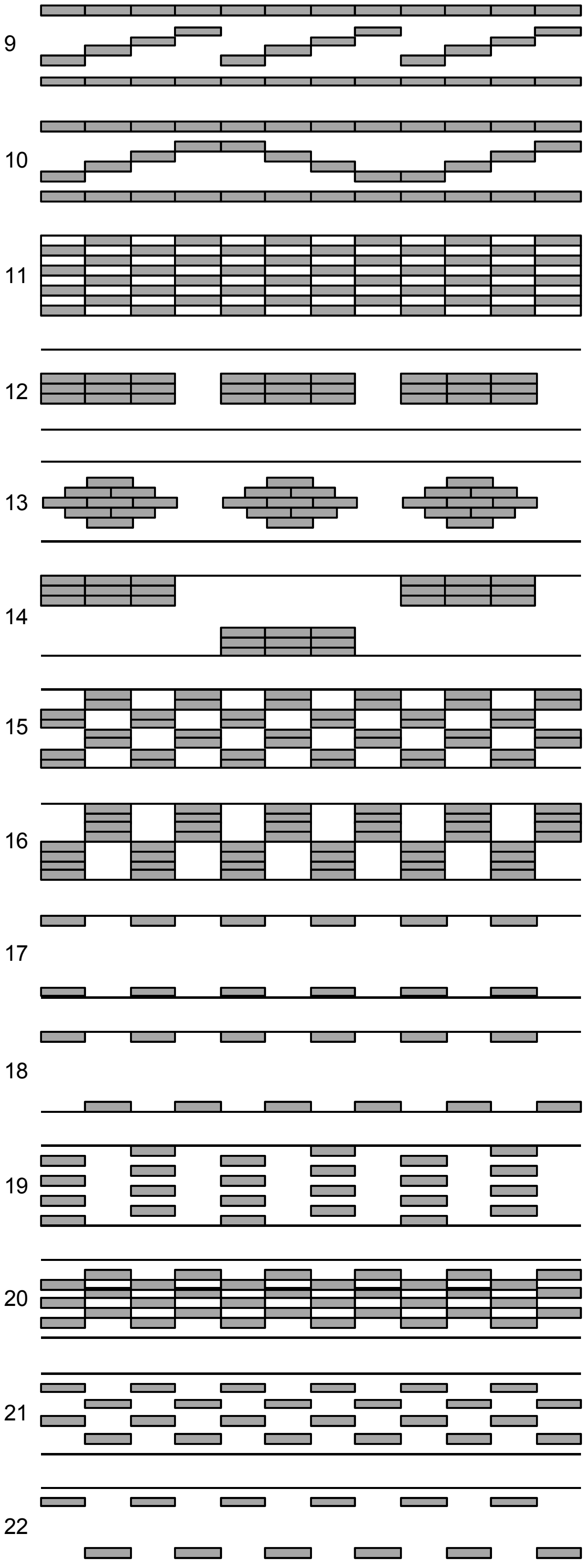

Figure 6. Emergent vegetation patch patterns investigated by James et al. (2001).

5 COMBINATION OF FORM AND SURFACE ROUGHNESS

Equations (5) to (7) have been tested experimentally for relatively sparse, large form roughness elements (such as boulders) in a channel. Experiments were conducted by Nkosi (2007) in the

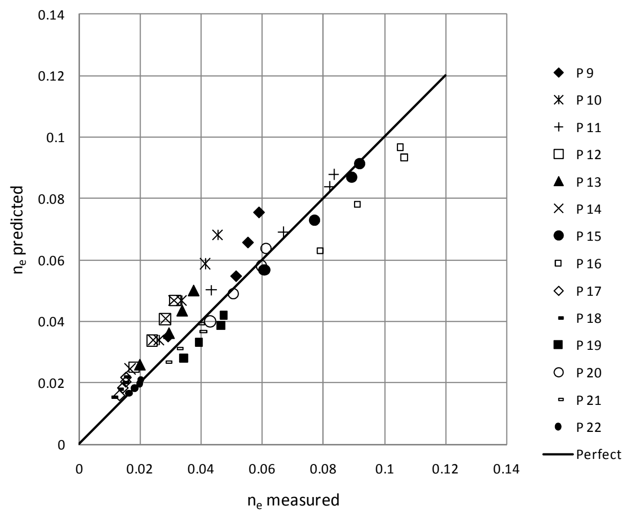

Figure 7. Comparison of measured and predicted overall Manning's n for vegetation patches.

same flume as used for the distributed surface roughness experiments. The form roughness elements were 0.11 m diameter circular cylinders set in staggered patterns with longitudinal and transverse centre spacings of 1.560 m, 1.100 m, 0.778 m and 0.55 m representing areal coverages (*Ac*) of 0.5%, 1%, 2% and 4% respectively. All arrangements were tested with the smooth flume surface (with a measured $n = 0.0107$) and also with a bed of 19 mm angular gravel (with a measured $n = 0.0270$).

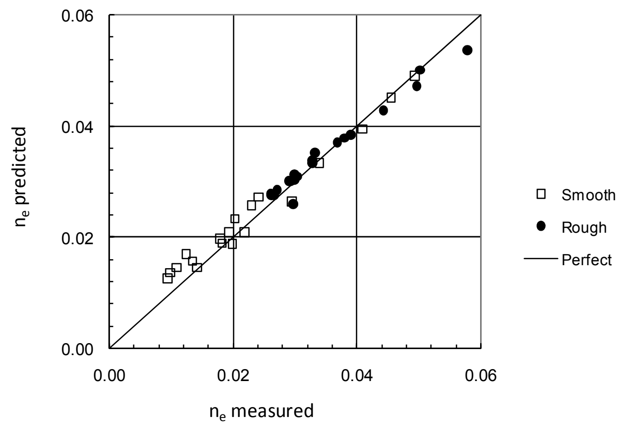

Figure 8. Comparison of measured and predicted overall Manning's *n* for combination of form and surface roughness.

In the predictions the value of C_D was selected to minimize the average absolute error in predicted discharge. The optimized value of 1.11 is realistic and produces average absolute errors in

n_e of 0.0021 for the smooth bed tests, 0.0012 for the rough bed tests and 0.0016 for all tests together. (Results are expressed in terms of Manning's *n* here for consistency.) The corresponding average absolute errors in discharge prediction are 11.2%, 3.29% and 7.12%. The predicted n_e values are compared with the measured values in Fig. 8.

6 IMPLICATIONS FOR CURRENT PRACTICE

Synthesis of a composite Manning's *n* as an average of local values weighted by plan area is realistic for spatially distributed surface roughness. The accuracy of predictions for calculating inbank channel conveyance is acceptable considering the uncertainty and variability of other input variables, especially the local *n* values. An analysis of the sensitivity to local *n* estimation of discharge as predicted by Eq. (2) with $K = A$ and $a = 1$ was carried out for the roughness patterns shown in Fig.1. This showed that changing the rough surface Manning *n* from 0.0216 by just +0.0021 and -0.0019 produced discrepancies from the original discharge predictions similar to the errors in the original predictions compared with the measured values.

There is some experimental evidence, however, that combinations of different resistance effects are not actually linear, and that the pattern of roughness distribution influences overall resistance. This is apparent in the surface roughness distributions shown in Fig. 1, where linear combination predictions deteriorate with increasing size and discreteness of patches. The effect is similar but more pronounced for the patches of emergent vegetation. The decreasing accuracy with increasing flows for some less well dispersed patterns suggests an emerging form resistance contribution from the patches as discrete elements. Features contributing to form resistance (such as emergent vegetation, boulders, and sudden changes in channel form) are common in rivers and particularly influential under low flow conditions.

The United States Soil Conservation Service (1963) method (Eq. (4)) is a particular application of linear superposition of resistance effects arising from both form and surface features. The inadequacy of this assumption can be demonstrated through application of Eqs. (5) to (7), which account for the two types of resistance deterministically. The situation described in Section 5 can be considered as a channel with a basic surface Manning's n_b and with the cylinders constituting an obstruction effect. In terms of Eq. (4), the overall resistance coefficient should then be given by $n_e = n_b + n_3$. For each of the experimental conditions the overall n_e was calculated from the measured discharge, slope and flow depth. The values of n_b were as measured for the smooth and rough surfaces. The value of n_3 necessary to produce the correct overall value was then calculated as $n_3 = n_e - n_b$. The required values of n_3 for all the experimental conditions are plotted against flow depth in Fig. 9. This shows that n_3 depends not only on the number and size of obstructions, but also on the basic n_b value and strongly on the flow depth. It cannot therefore be considered as a unique, independent, variable, making its estimation from tabular or photographic guides unreliable. Equation (4) therefore does not provide a sound basis for synthesizing a composite resistance coefficient in practice where features that induce form type resistance are present.

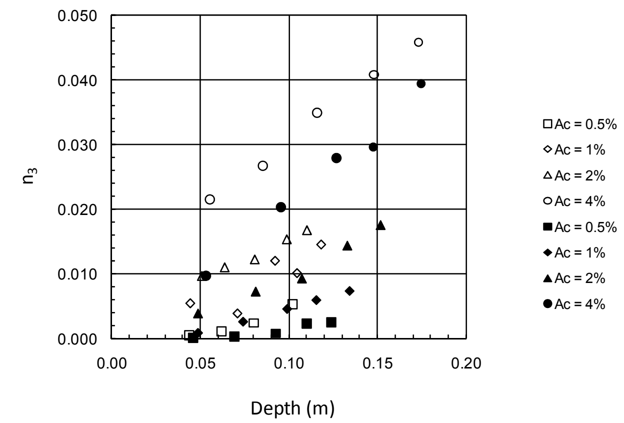

Figure 9. Dependence of Manning's *n* modifying factor for obstructions on flow depth, bed roughness and obstruction density. (Open markers are for smooth bed tests, closed markers are for rough bed tests.)

Equation (3) also provides for combining surface and form resisting effects, but using independent local resistance coefficients rather modifying factors. The approach of calculating the square root of the sum of squares of contributing values can be shown to be consistent with Eq. (5) by separating the form and surface resistance components and expressing them in terms of equivalent Manning's *n* values. This approach has been tested against the combined surface and form resistance data in the same way as for Eq. (4) above. The combined coefficient value can be expressed as $n_l = (n_{form}^2 + n_{sur}^2)^{0.5}$, where n_{form} accounts for the form resistance contribution. The values of n_{form} required to produce the correct overall values are plotted against flow depth in Fig. 10. In this case the values for tests with the smooth and rough beds coincide closely, indicating that the combination equation allows n_{form} to be considered as a unique variable independent of the bed roughness. It must be noted that Eq. (3) does not account explicitly for the relative preponderance of the different contributing resistance characteristics, whereas Eq. (5) does so through the form roughness element size and density. Estimation of the constituent values in Eq. (3) must therefore consider their relative contributions using other information. Equations (3) and (5) can be considered as expressions of Eq. (1) with $a = 2$, with the weighting accounted for deterministically by Eq. (5) but not explicitly accounted for by Eq. (3). Use of Eq. (3) also requires inclusion of the effect of flow depth on constituent values, whereas Eq. (5) accounts for this effect deterministically. The form of Eq. (3) does, however, provide a sounder base for combining resistance contributions, and should be preferred over Eq. (4) in future developments.

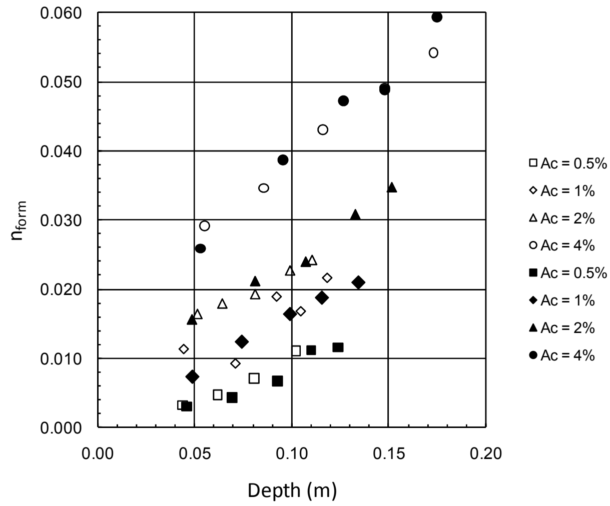

Figure 10. Dependence of n_{form} on flow depth and obstruction density. (Open markers are for smooth bed tests, closed markers are for rough bed tests.)

7 CONCLUSIONS

The effective resistance of a channel comprising surfaces with different roughnesses can be satisfactorily described through a combination of Manning's resistance coefficients for the different surfaces, weighted by their contributing surface areas (Eq. (2) with $K = A$).

For surface resistance conditions, values of the exponent on local n values (a) of 2, 3/2 and 1 are equally effective.

The same approach can be used with $a = 1$ for channels with patches of emergent vegetation, but accuracy decreases as patches become larger and less uniformly dispersed.

Equation (2) with $K = P$ can be used for channels with emergent bank vegetation, but the resistance coefficient of the stem-water interface varies considerably with channel and flow conditions and should be accounted for (e.g. through Eq. (8)).

Form resistance is not well described by conventional resistance equations. Equations (5) to (7) provide an effective means of combining bed surface resistance with form contributions from discrete elements such as boulders.

The United States Soil Conservation Service (1963) approach of augmenting a basic value of n associated with the bed surface to account for other effects is not recommended because the modifying factors are not independent.

The local combination equation proposed by HR Wallingford (2004) is sound but requires subjective accounting for the relative preponderance of different effects.

Whatever combination procedure is applied, accuracy depends primarily on reliable estimation of the constituent n values.

REFERENCES

Bhembe, S.S., Pandey, S.V.G. 2006. Composite roughness in open-channel flow. Investigational Project Report, School of Civil & Environmental Engineering, University of the Witwatersrand, South Africa.

Cowan, W. L. 1956. Estimating hydraulic roughness coefficients. Agricultural Engineering, 37(7), 473-475.

Fisher, K.R. 1993. Spatial variations of in-bank hydraulic roughness in channels, Report SR 357, HR Wallingford, UK.

Hirschowitz, P.M., James, C.S. 2009. Conveyance estimation in channels with emergent bank vegetation, Water SA, 35(5), 607-613.

Horton, R.E. 1933. Separate roughness coefficients for channel bottom and sides. Engineering News Record, III(22), 652-653.

HR Wallingford. 2004. Reducing uncertainty in river flood conveyance, Phase 2, Conveyance Manual. Defra/Environment Agency Project W5A-057, United Kingdom.

James, C.S., Birkhead, A.L., Jordanova, A.A., Kotschy, K.A., Nicolson, C.R., Makoa, M.J. 2001. Interaction of reeds, hydraulics and river morphology, Report No. 856/1/01, Water Research Commission, Pretoria, South Africa.

James, C.S., Goldbeck, U.K., Patini, A., Jordanova, A.J. 2008. Influence of foliage on flow resistance of emergent vegetation, Journal of Hydraulic Research, 46(4), 536-542.

James, C.S., Makoa, M. J. 2006. Conveyance estimation for channels with emergent vegetation boundaries, Proceedings of the Institution of Civil Engineers, Water Management, 159(WM4), 235-243.

Kaiser, W. 1984. Fließwiderstandsverhalten in Gerinnen mit durchströmten Ufergehölzzonen. Wasserbau-Mitteilung der Technische Hochschule Darmstadt, Darmstadt, Germany, Vol. 23.

Nkosi, M.M. 2007. Flow resistance effect of large-scale roughness elements. Investigational Project Report, School of Civil & Environmental Engineering, University of the Witwatersrand, South Africa.

Pavlovski, N.N. 1931. On a design formula for uniform flow movement in channels with non-homogeneous walls. Transactions of All-Union Scientific Research In-

stitute of Hydraulic Engineering, Leningrad, 3, 157-164 (in Russian).
United States Soil Conservation Service. 1963. Guide for Selecting Roughness Coefficient 'n' Values for Channels. United States Department of Agriculture, Soil Conservation Service, Washington, D.C.